



HAL
open science

Elastocaloric properties of thermoplastic polyurethane

Gildas Coativy, Hiba Haissoune, Laurence Seveyrat, Gaël Sebald, Laurent Chazeau, Jean-Marc Chenal, Laurent Lebrun

► **To cite this version:**

Gildas Coativy, Hiba Haissoune, Laurence Seveyrat, Gaël Sebald, Laurent Chazeau, et al.. Elastocaloric properties of thermoplastic polyurethane. Applied Physics Letters, 2020, 117 (19), pp.193903. 10.1063/5.0023520 . hal-03205385

HAL Id: hal-03205385

<https://insa-lyon.hal.science/hal-03205385>

Submitted on 11 Apr 2022

HAL is a multi-disciplinary open access archive for the deposit and dissemination of scientific research documents, whether they are published or not. The documents may come from teaching and research institutions in France or abroad, or from public or private research centers.

L'archive ouverte pluridisciplinaire **HAL**, est destinée au dépôt et à la diffusion de documents scientifiques de niveau recherche, publiés ou non, émanant des établissements d'enseignement et de recherche français ou étrangers, des laboratoires publics ou privés.

Elastocaloric properties of thermoplastic polyurethane

Gildas Coativy^a, Hiba Haissoune^{a,c}, Laurence Seveyrat^a, Gaël Sebald^{a,b}, Laurent Chazeau^c,
Jean-Marc Chenal^c, Laurent Lebrun^a

^a Univ Lyon, INSA-Lyon, LGEF, EA682, F-69621, Villeurbanne, France

^b ELYTMaX UMI 3757, CNRS, Université de Lyon, Tohoku University, International Joint
Unit, Tohoku University, 980-8577 Sendai, Japan

^c Univ Lyon, INSA-Lyon, CNRS, MATEIS, UMR 5510, F-69621 Villeurbanne, France

corresponding author : Gildas Coativy email address : gildas.coativy@insa-lyon.fr

Abstract

Very few studies have explored the elastocaloric effect of elastomers other than natural rubber (NR). The aim of the present article is thus to evaluate the elastocaloric properties of a thermoplastic polyurethane (TPU) in terms of microstructural characteristics and thermoelastic coupling. Calorimetric measurements showed two successive peaks at 240 K and 282 K, attributed to respectively the crystallization and melting of soft segments. X-ray diffraction indicated that TPU exhibited a fully reversible strain-induced crystallization (SIC) at room temperature. Thermomechanical experiments performed at different elongations revealed a minimum adiabatic temperature variation of about -8 K after retraction of a sample initially elongated at $\lambda=5$. This is comparable to NR performances. However, for cycles carried out between $\lambda=1$ and $\lambda=5$, tensile stress/elongation curves showed a non-elastic behavior of TPU. A pseudo-elastic response was obtained for cyclic elongation when unloading was incomplete, in our case when λ was between 3 and 5. The recorded peak-to-peak temperature variation decreased from 4.5 K to 3.3 K when the number of cycles was increased to 5000. Despite that the issue of fatigue resistance for TPU needs to be addressed, this work opens new perspectives for studying the elastocaloric properties of various polyurethanes (whether crosslinked or thermoplastic) as well as other materials with a tendency for strain-induced crystallization, such as polychloroprene, hydrogenated acrylonitrile butadiene rubber and others.

Keywords: polyurethane, elastocaloric effect, fatigue, infrared imaging, thermoplastic elastomer

32 The development of caloric materials is an active research area dedicated to replacing coolants
33 used in cooling systems.^{1,2} Basically, caloric materials can become structurally
34 ordered/disordered upon the application/removal of an electric or magnetic field or a
35 mechanical stress.^{1,3-5} The resulting order/disorder transitions are responsible of entropy
36 variations. When these transitions are faster than the time needed for the material to exchange
37 heat with its surroundings, there occurs a positive or negative temperature variation of the
38 material.¹ Among elastocaloric materials, elastomers are of interest due to their elastocaloric
39 effect being triggered by small stress values (a few MPa) and the associated significant
40 temperature variations which can reach 14 K.⁶⁻⁹ In addition, they are cheap materials. For these
41 reasons, the use of elastomers in solid-state cooling systems is gaining widespread interest in
42 several scientific communities,^{9,10} and strongly motivates studying the elastocaloric effect of
43 various elastomers.

44 The elastocaloric effect is mainly attributed to two contributions:^{6-8,11,12} the first is a reversible
45 orientation/disorientation of macromolecules in the strain direction (entropic elasticity),¹¹
46 which can be observed in all amorphous elastomers. The second contribution is strain-induced
47 crystallization (SIC) that corresponds to a partial crystallization of the elastomer as a result of
48 the deformation.

49 Depending on the initial structure of the elastomer (crosslink density, crosslink distribution...)
50 and the mechanical stress program that is applied, the elastocaloric effect can be either
51 reversible or irreversible. For instance, the stretching of natural rubber (NR) with a low
52 crosslink density can lead to the formation of crystals that are stable at room temperature
53 whereas with an intermediate crosslink density, the formed crystals are unstable and melt when
54 the stress is released.¹³⁻¹⁶ The elastocaloric effect of NR has been well documented and it has
55 been revealed that the dominant caloric effect is the reversible SIC.^{6,7} However, although SIC
56 is observed in other elastomers such as polyurethane, hydrogenated acrylonitrile butadiene
57 rubber (HNBR) and polychloroprene¹⁷⁻²⁴, the elastocaloric effect of these materials has yet to
58 be investigated.

59 The motivation for the work presented here is to display an elastocaloric effect in thermoplastic
60 elastomers (TPE). These heteropolymers are made of hard segments (HS) (with a melting
61 temperature T_m or a glass transition temperature T_g above room temperature T_{room}) and soft
62 segments (SS) that are in the rubbery state at T_{room} .²⁵ These HS and SS are covalently bonded,
63 but their partial or total immiscibility is responsible for a phase-separated structure made of HS-
64 and SS-rich domains. The HS-rich domains play the role of physical crosslinks at T_{room}

65 permitting the elastomeric behavior of SS in TPE, while above T_m , the TPE can be melt
66 processed due to the melting of the HS-rich domains. This melt processability can be
67 advantageous for making complex hermetic systems at lab scale for testing elastocaloric devices
68 such as regenerative systems incorporating a fluid.¹⁰

69 Previous investigations have brought to light the strain-induced crystallization (SIC) of
70 crosslinked and thermoplastic polyurethanes (TPU) using calorimetry and X-ray diffraction
71 (XRD).^{20–24} The main objective of this work is to evidence the reversible SIC of the TPU chosen
72 for this study by the aforementioned techniques and the second aim is to study the elastocaloric
73 effect of TPU by stretching the samples rapidly at $1600\%.s^{-1}$ and measuring the temperature
74 variation. The final goal is to explore the cyclic elastocaloric behavior of TPU over 5000 cycles.

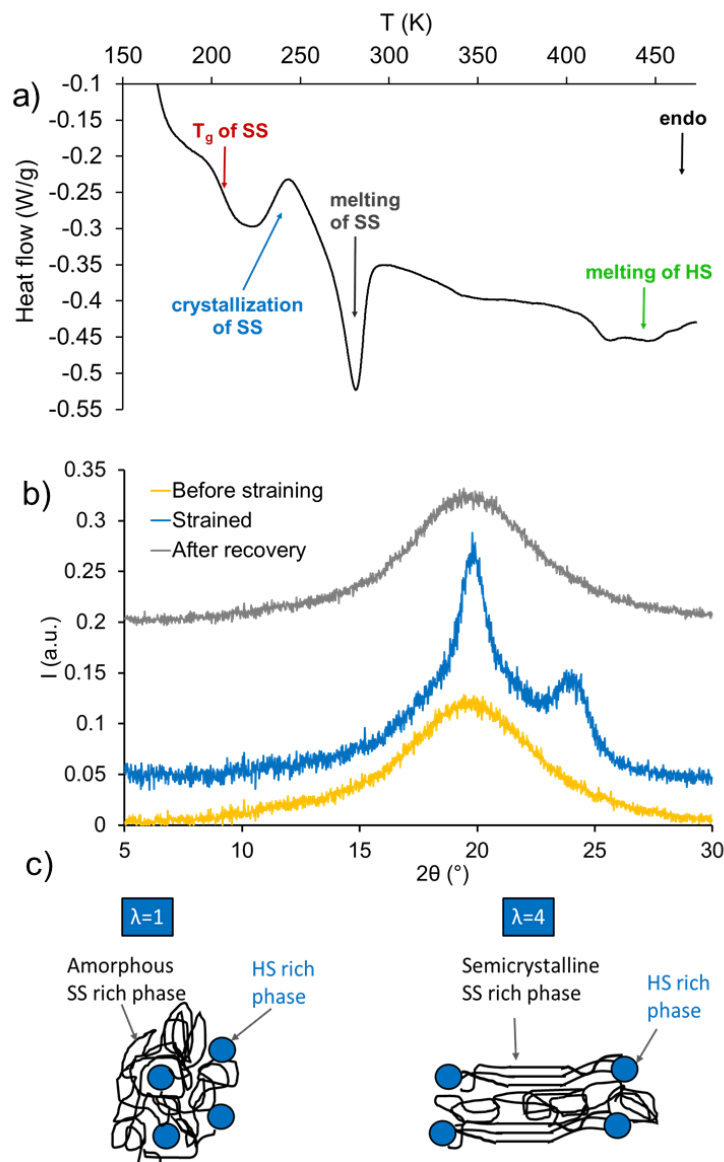
75 The investigated material is an aromatic polyether-based thermoplastic polyurethane Estane®
76 X4977 NAT 039 grade from Lubrizol. TPU is composed of poly(tetramethylene-oxide)
77 (PTMO) with a molecular weight of 2000 g/mol as soft segments (SS) and 4,4'-methylene-bis-
78 (phenyl-isocyanate) (MDI) and 1,4-butanediol (BDO) as hard segments (HS). Due to phase
79 separation, the HS formed highly polar and stiff microdomains embedded in a soft poorly polar
80 matrix.²⁶ The same procedure as the one described by Jomaa et al. was used to prepare a TPU
81 film by solvent casting.²⁶ In short, TPU granules were dissolved in dimethylformamide (DMF)
82 at a ratio of 25wt%. After being heated up to 353 K for 4h, the solution was cast onto a glass
83 plate with an Elcometer 3700 film applicator. The films were then dried at 333 K for 24h and
84 annealed at 398 K for 3 hours. Their final thickness is about 200 μm .

85 X-ray diffraction measurements were carried out at room temperature with an XPert Pro MPD
86 Panalytical diffractometer equipped with a graphite monochromator ($\text{CuK}\alpha 1$ radiation) and a
87 X'Celerator detector. For the measurement under strain, the samples were manually stretched
88 and fixed to the sample holder during their deformation. The calorimetric analysis was
89 performed by Differential Scanning Calorimetry (Setaram, DSC 131 evo) under nitrogen
90 atmosphere. The samples (about 20 mg) were placed in closed aluminum crucibles and cooled
91 from ambient temperature down to 153 K, then heated to 488 K and finally cooled. The heating
92 and cooling ramps were carried out at $10\text{ K}\cdot\text{min}^{-1}$. The elastocaloric coupling of TPU samples
93 ($20*20*0.2\text{ mm}^3$) was investigated via a tensile test bench combined with an infrared camera
94 similar to the one used by Yoshida et al.²⁷ The tensile test bench was composed of a single axis
95 robot RSDG212 (MISUMI Corporation, Japan) with an analog force sensor XFTC300-200N
96 (Measurement Specialties, France). The displacement was measured with a laser optical
97 displacement sensor ILD1420-200 (micro-epsilon, France) and the corresponding elongation

98 $\lambda = \frac{l(t)}{l_0}$ was defined as the ratio between the length l at time t and the initial length $l_0=20$ mm.

99 In parallel, the material's surface temperature was measured using a thermal camera Optris
100 PI450 (Optris, Germany).

101 Figure 1(a) presents the thermogram of TPU after processing. The glass transition temperature
102 of the soft segments T_{gss} is visible at 205 K. The peaks observed at 240 K and at 282 K (just
103 below room temperature) could be attributed to the partial crystallization and the melting of SS,
104 respectively.^{26,28} The enthalpy of melting is about 17 kJ/kg. The double peaks at 424 K and 445
105 K could either correspond to the melting of the semicrystalline HS with two different chain
106 lengths, or be related to rearrangements within SS and HS followed by the fusion of crystalline
107 HS.²⁶ In summary, below the glass transition temperature of the soft segments ($T_{gss}=205$ K),
108 the material is mainly made up of amorphous SS-rich phases and semicrystalline HS-rich
109 phases, whereas above T_{gss} , the SS phase crystallizes partially around 240 K until reaching 273
110 K and melts just below room temperature (at around 282 K), thus reverting to the initial structure
111 made of amorphous SS domains and semicrystalline HS-rich phases.



112

113 FIG. 1. (a) DSC thermogram of TPU. (b) X-ray diffractograms of TPU before, during and
 114 after straining at $\lambda=4$. (c) Schematic of strain-induced crystallization of TPU

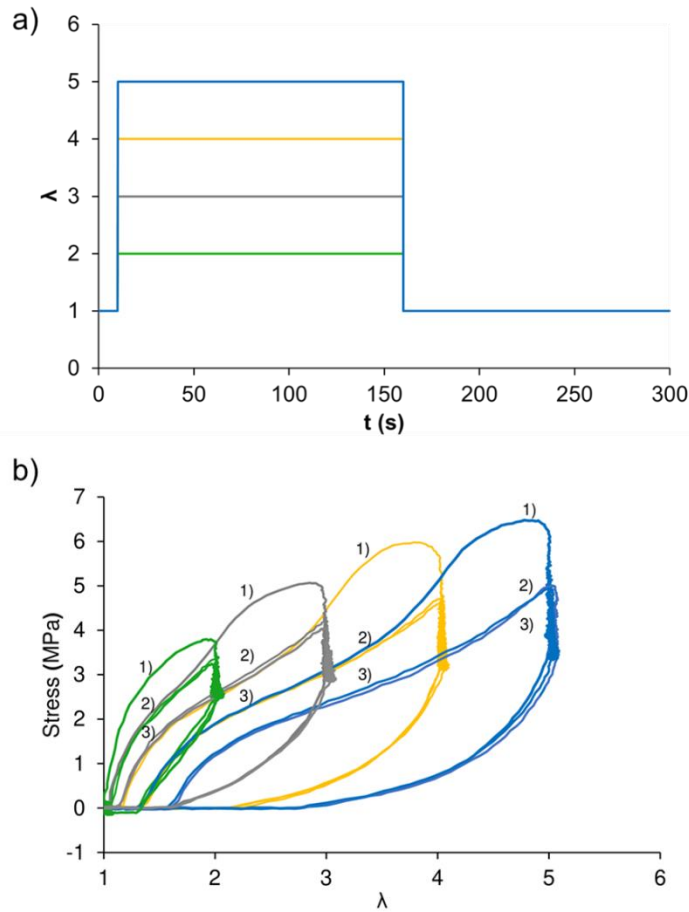
115 This experiment suggests that the soft segments, not subjected to any strain, are amorphous at
 116 room temperature. X-ray diffraction was performed on the TPU before, during and after
 117 stretching at $\lambda=4$ (Fig. 1(b)). Although the hard domains were not melted, an amorphous halo
 118 was observed at $\lambda=1$ for the unstretched sample. It was centered at $2\theta=20^\circ$ and had a shoulder
 119 at $2\theta=12^\circ$. When the material was stretched up to $\lambda=4$, two diffraction peaks appeared at
 120 $2\theta=19.8^\circ$ and $2\theta=24.1^\circ$. According to Ren et al, this is evidence of strain-induced crystallization
 121 (SIC) of the PTMO soft segments as depicted in Fig. 1(c).²³ These results are in good agreement
 122 with the X-ray diffraction pattern of pure PTMO.²⁹ Furthermore, when the stress was released,
 123 the X-ray pattern exhibited an amorphous halo once again thus demonstrating the reversibility
 124 of the SIC at room temperature.

125 It is worth mentioning that the presence of a melting peak at a temperature between 273 K and
126 283 K and the ability of the elastomer to crystallize under strain at room temperature has also
127 been observed in other elastomers such as natural rubber (NR), hydrogenated acrylonitrile
128 butadiene rubber (HNBR) or polychloroprene.^{17-19,30,31} The presence of such a melting peak
129 could be an indicator of a reversible SIC in the elastomers. In the case of SIC, the orientation
130 of the macromolecules in the strain direction causes an entropy reduction of the
131 macromolecules conformation which shifts the crystallization and melting temperatures
132 towards a higher value.¹⁵ However, after releasing the stress completely, the melting
133 temperature drops, leading to the complete melting of the crystals.

134 The occurrence of SIC in TPU suggests a strong elastocaloric effect. In order to estimate the
135 adiabatic temperature variation, TPU was strained adiabatically at different elongations from
136 $\lambda=1$ to λ_f (Fig. 2(a)) according to the following:

137 The first step consisted in stretching the TPU at 320 mm.s^{-1} ($1600\%.\text{s}^{-1}$), after which the material
138 was maintained at constant elongation during 150 s. When thermal equilibrium was reached,
139 the elongation was decreased back to $\lambda=1$ at 320 mm.s^{-1} , and kept there until reaching thermal
140 equilibrium again.

141 TPU exhibited fatigue during the first cycles as evidenced in Fig. 2(b) which displays the
142 stress/elongation curves of the first three mechanical cycles of TPU elongated to various final
143 elongations, i.e., $\lambda_f = 2, 3, 4$ and 5 .



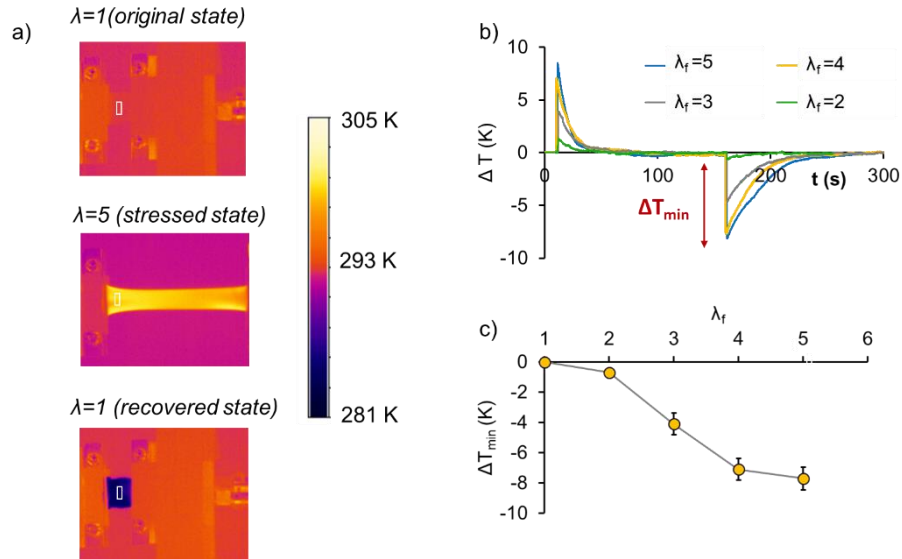
144

145 FIG. 2. Mechanical testing of TPU. (a) The mechanical stress program. (b) The evolution of
 146 the stress as a function of elongation (first 3 cycles).

147

148 For each mechanical test, the first cycle differs from the second and third cycles in that it
 149 presents a higher stress but the same remanent elongation. This is probably due to the structural
 150 modification of the HS structure.³² Indeed, it can be noted that the mechanical response exhibits
 151 both elastic and inelastic parts and when the elongation increases, so does the inelastic part. The
 152 third cycle is similar to the second, suggesting that the mechanical behavior becomes stabilized.
 153 The maximum stress of the third cycle ranges from 3 MPa to 5 MPa, for a maximum elongation
 154 varying between 2 and 5.

155 Moreover, during the third mechanical cycle, the temperature of the sample surface was
 156 measured with an IR camera in the white rectangle represented in Fig. 3(a). The resulting
 157 temperature variation ΔT as a function of time is reported in Fig. 3(b).



158

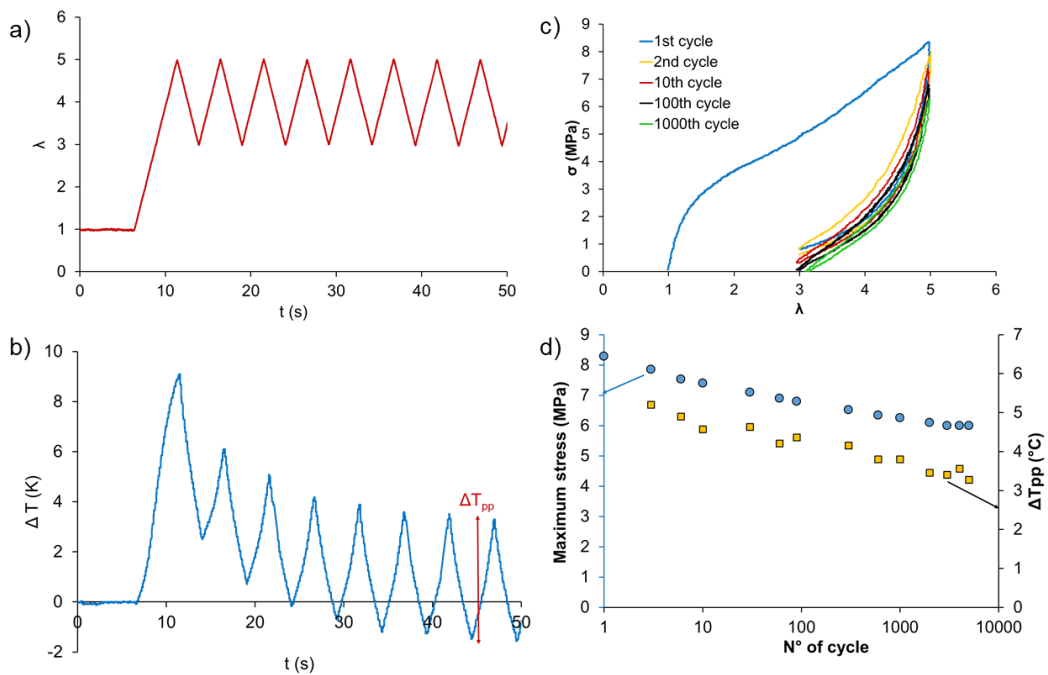
159 FIG. 3. Elastocaloric properties of polyurethane. (a) IR images for three states: $\lambda=1$ (original
 160 state), $\lambda=5$ (stressed state) and $\lambda=1$ (recovered state) of TPU (b) Temperature variation as a
 161 function of time ($\Delta T = T(t) - T_{room}$). (c) The minimum temperature variation ΔT_{min} as a function
 162 of the final elongation λ_f .

163 The fast stretching of the material induces a positive temperature variation ΔT caused by SS
 164 orientation and crystallization. At constant elongation the temperature drops until reaching
 165 thermal equilibrium. Then, a return to the initial elongation at $\lambda=1$ leads to a decrease of ΔT
 166 induced by disorientation of the soft segments and melting of the crystals. Moreover, the width
 167 of these two peaks varies. It becomes narrower after elongation than after retraction due to the
 168 stretched sample becoming thinner in comparison with the initial thickness at $\lambda=1$. The
 169 thickness reduction of the sample favors heat transfer.³²

170 Regarding the elastocaloric effect, $|\Delta T_{min}|$ increases significantly (from 1 K to 7.1 K) for a
 171 final elongation λ_f between 2 and 4 and slightly (from 7.1 K to 7.7 K) when λ_f varies between
 172 4 and 5 (Fig. 3(c)). This onset of saturation could be explained by a higher inelastic mechanical
 173 response when λ_f increases. Finally, the temperature variation is within the same range as that
 174 of natural rubber (NR) at $\lambda_f=5$ whereas for lower elongations, the adiabatic temperature
 175 variation is higher for TPU.^{7,8}

176 Cyclic elastocaloric properties were studied by imposing a triangular cyclic elongation between
 177 $\lambda=3$ and $\lambda=5$ (Fig. 4(a)). With a chosen frequency $f=0.2$ Hz, 5000 cycles could be applied
 178 without the sample breaking. The resulting temperature variation is presented in Fig. 4(b). The
 179 peak-to-peak temperature variation ΔT_{pp} varies between 4.5 K and 3.3 K (Fig. 4(d)) when the
 180 number of cycle increases from 10 to 5000. It corresponds to a decrease of about 10% per
 181 decade. It can be noted that ΔT_{pp} for TPU is in the same range as for NR when the latter is
 182 cycled between $\lambda=3$ and $\lambda=6$ ³³, but with a lower stability.

183



184

185 FIG. 4. Elastocaloric effect of polyurethane during triangular solicitation when λ was varied
 186 between 3 and 5 at $f=0.2$ Hz. (a) Elongation program. (b) Temperature variation as a function
 187 of time. (c) Stress/elongation curves of TPU for a varying number of cycles. (d) Maximum
 188 stress and peak-to-peak temperature variation as a function of the number of cycles.

189 Figure 4(c) shows the stress/elongation curves of TPU for a varying number of cycles. With the
 190 exception of the first cycle, the hysteresis loss is about 1 kJ/kg per cycle. The maximum stress
 191 and the peak-to-peak temperature variation ΔT_{pp} decrease when the number of cycles increases
 192 (Fig. 4(d)). After the hundredth cycle, the stress at $\lambda=3$ is equal to 0 MPa, indicating an inelastic
 193 response. Besides, an estimation of heat exchange can be obtained according to $Q \approx c \Delta T_{pp} = 8$
 194 kJ/kg (where c is the specific heat capacity of TPU). This is 8 times larger than the mechanical
 195 losses in a single cycle. An indicator of material performance of a cooling device using a caloric

196 material is the coefficient of performance COP, defined roughly as $COP_{\text{mat}}=Q/W_{\text{losses}}$. The COP
197 value of 8 obtained here is in the normal range of caloric materials, i.e., between 5 and 20.^{34,35}

198 To sum up, this work investigated the elastocaloric properties of thermoplastic polyurethane. A
199 strain-induced crystallization was revealed via X-ray diffraction, and it was verified that the
200 crystals melted after complete unloading, indicating a fully reversible strain-induced phase
201 transition. Consequently, the latent heat of this phase transformation contributed fully to the
202 elastocaloric effect after complete unloading. The adiabatic mechanical tests exhibited a
203 temperature variation in the same range as that found for natural rubber when tested under
204 identical conditions.

205 The mechanical and elastocaloric fatigue tests demonstrated that a large elastocaloric effect
206 ($\Delta T_{\text{pp}} > 3\text{K}$) could be maintained for 5000 cycles. From a system point of view, it should be
207 noted that thermoplastic polyurethane can be melt processed or potentially 3D printed, opening
208 great perspectives in terms of fabrication and optimization of cooling devices at a lab scale.
209 Such cooling systems could also be advantageous for testing analytical or numerical models of
210 elastocaloric devices with a variety of complex shapes that can be practically produced.
211 However, from an applicative viewpoint, the continuous decrease of elastocaloric properties
212 and the inelastic response of TPU are limiting factors for solid state cooling applications. To
213 address these issues and increase the panel of elastocaloric polymers, other polyurethanes, such
214 as crosslinked polyurethane with varying HS/SS ratios, or other elastomers, such as HNBR or
215 polychloroprene, should be studied.¹⁷⁻²⁴

216

217 Acknowledgement

218

219 This work was supported by ANR through the project ECPOR (No. ANR-17-CE05-0016) The
220 authors gratefully acknowledge the French Region Auvergne-Rhône-Alpes, the French project
221 IDEXLYON of the Université de Lyon in the framework of the “Investissements d’Avenir”
222 program (No. ANR-16-IDEX-0005). The authors would also like to thank Dr. Sandrine
223 Cardinal for her help with the X-ray diffraction experiments.

224 Data availability

225 The data that support the findings of this study are available from the corresponding authors
226 upon reasonable request.

227 References

228
229 ¹ I. Takeuchi and K. Sandeman, *Phys. Today* **68**, 48 (2015).
230 ² L. Mañosa and A. Planes, *Appl. Phys. Lett.* **116**, 050501 (2020).
231 ³ A. Chauhan, S. Patel, R. Vaish, and C.R. Bowen, *MRS Energy Sustain.* **2**, E16 (2015).
232 ⁴ X. Moya, S. Kar-Narayan, and N.D. Mathur, *Nat. Mater.* **13**, 439 (2014).
233 ⁵ E.O. Usuda, N.M. Bom, and A.M.G. Carvalho, *Eur. Polym. J.* **92**, 287 (2017).
234 ⁶ J.C. Mitchell and D.J. Meier, *J. Polym. Sci. Part A-2 Polym. Phys.* **6**, 1689 (1968).
235 ⁷ Z. Xie, C. Wei, D. Guyomar, and G. Sebald, *Polymer (Guildf)*. **103**, 41 (2016).
236 ⁸ S.L. Dart, R.L. Anthony, and E. Guth, *Ind. Eng. Chem.* **34**, 1340 (1942).
237 ⁹ R. Wang, S. Fang, Y. Xiao, E. Gao, N. Jiang, Y. Li, L. Mou, Y. Shen, W. Zhao, S. Li, A.F.
238 Fonseca, D.S. Galvão, M. Chen, W. He, K. Yu, H. Lu, X. Wang, D. Qian, A.E. Aliev, N. Li,
239 C.S. Haines, Z. Liu, J. Mu, Z. Wang, S. Yin, M.D. Lima, B. An, X. Zhou, Z. Liu, and R.H.
240 Baughman, *Science (80-.)*. **366**, 216 (2019).
241 ¹⁰ G. Sebald, A. Komiya, J. Jay, G. Coativy, and L. Lebrun, *J. Appl. Phys.* **127**, 094903
242 (2020).
243 ¹¹ J. Pellicer, J.A. Manzanares, J. Zúñiga, P. Utrillas, and J. Fernández, *J. Chem. Educ.* **78**,
244 263 (2001).
245 ¹² G.A. Holzapfel and J.C. Simo, *Comput. Methods Appl. Mech. Eng.* **132**, 17 (1996).
246 ¹³ B. Heuwers, A. Beckel, A. Krieger, F. Katzenberg, and J.C. Tiller, *Macromol. Chem. Phys.*
247 **214**, 912 (2013).
248 ¹⁴ B. Heuwers, D. Quitmann, F. Katzenberg, and J.C. Tiller, *Macromol. Rapid Commun.* **33**,
249 1517 (2012).
250 ¹⁵ N. Candau, R. Laghmach, L. Chazeau, J.-M. Chenal, C. Gauthier, T. Biben, and E. Munch,
251 *Macromolecules* **47**, 5815 (2014).
252 ¹⁶ J.M. Chenal, C. Gauthier, L. Chazeau, L. Guy, and Y. Bomal, *Polymer (Guildf)*. **48**, 6893
253 (2007).
254 ¹⁷ K.N. Ulu, M. Dragičević, P.-A. Albouy, B. Huneau, A.-S. Béranger, and P. Heuillet, in
255 *Const. Model. Rubber X* (CRC Press, 2017), pp. 279–282.
256 ¹⁸ G. Severe and J.L. White, *J. Appl. Polym. Sci.* **78**, 1521 (2000).
257 ¹⁹ P.-Y. Le Gac, P.-A. Albouy, and D. Petermann, *Polymer (Guildf)*. **142**, 209 (2018).
258 ²⁰ H. Koerner, J.J. Kelley, and R.A. Vaia, *Macromolecules* **41**, 4709 (2008).
259 ²¹ F. Yeh, B.S. Hsiao, B.B. Sauer, S. Michel, and H.W. Siesler, *Macromolecules* **36**, 1940
260 (2003).
261 ²² K. Kojio, S. Nakamura, and M. Furukawa, *Polymer (Guildf)*. **45**, 8147 (2004).
262 ²³ L. Ren, P.N. Shah, and R. Faust, *J. Polym. Sci. Part B Polym. Phys.* **54**, 2485 (2016).
263 ²⁴ W. Gabriëlse, M. Soliman, and K. Dijkstra, *Macromolecules* **34**, 1685 (2001).

- 264 ²⁵ R.J. Spontak and N.P. Patel, *Curr. Opin. Colloid Interface Sci.* **5**, 333 (2000).
- 265 ²⁶ M.H. Jomaa, K. Masenelli-Varlot, G. Diguët, L. Seveyrat, L. Lebrun, K. Wongtimnoi, C.
266 Vechambre, J.M. Chenal, and J.Y. Cavallé, *Polymer (Guildf)*. **62**, 139 (2015).
- 267 ²⁷ Y. Yoshida, K. Yuse, D. Guyomar, J.-F. Capsal, and G. Sebald, *Appl. Phys. Lett.* **108**,
268 242904 (2016).
- 269 ²⁸ N.S. Schneider and C.S.P. Sung, *Polym. Eng. Sci.* **17**, 73 (1977).
- 270 ²⁹ C. Wang, C. Ma, C. Mu, and W. Lin, *RSC Adv.* **7**, 27522 (2017).
- 271 ³⁰ J.M. Chenal, L. Chazeau, Y. Bomal, and C. Gauthier, *J. Polym. Sci. Part B Polym. Phys.*
272 **45**, 955 (2007).
- 273 ³¹ G.T. Ovanesov, A.M. Mashuryan, K.A. Gasparyan, V.G. Baranov, and S.Y. Frenkel,
274 *Polym. Sci. U.S.S.R.* **28**, 1174 (1986).
- 275 ³² P.H. Mott, C.B. Giller, D. Fragiadakis, D.A. Rosenberg, and C.M. Roland, *Polymer*
276 *(Guildf)*. **105**, 227 (2016).
- 277 ³³ G. Sebald, Z. Xie, and D. Guyomar, *Philos. Trans. R. Soc. London A Math. Phys. Eng. Sci.*
278 **374**, 439 (2016).
- 279 ³⁴ S. Qian, Y. Geng, Y. Wang, J. Ling, Y. Hwang, R. Radermacher, I. Takeuchi, and J. Cui,
280 *Int. J. Refrig.* **64**, 1 (2016).
- 281 ³⁵ J. Cui, Y. Wu, J. Muehlbauer, Y. Hwang, R. Radermacher, S. Fackler, M. Wuttig, and I.
282 Takeuchi, *Appl. Phys. Lett.* **101**, 073904 (2012).
- 283